Optics and Photonics Journal, 2023, 13, 147-155
https://www.scirp.org/journal/opj
ISSN Online: 2160-889X
ISSN Print: 2160-8881

Green Synthesis and Luminescent Properties of Mn^{4+} Doped Red Phosphor for WLED

Xiaoyi Liu[1,2], Guixia Liu[1,2*]

[1]College of Materials Science and Engineering, Changchun University of Science and Technology, Changchun, China
[2]Key Laboratory of Applied Chemistry and Nanotechnology at Universities of Jilin Province, Changchun University of Science and Technology, Changchun, China
Email: *liuguixia22@163.com

How to cite this paper: Liu, X.Y. and Liu, G.X. (2023) Green Synthesis and Luminescent Properties of Mn^{4+} Doped Red Phosphor for WLED. *Optics and Photonics Journal*, **13**, 147-155.
https://doi.org/10.4236/opj.2023.136013

Received: March 16, 2023
Accepted: June 27, 2023
Published: June 30, 2023

Abstract

Herein, the $K_3MoO_2F_5{\cdot}2H_2O{:}Mn^{4+}$ phosphor was synthesized by using low toxic NH_4HF_2 and HCl instead of highly toxic HF. The $K_3MoO_2F_5{\cdot}2H_2O{:}Mn^{4+}$ phosphor has a blocky structure and exhibits sharp red emission at the range of 580 to 670 nm excited by the blue light at 470 nm. The fabricated WLED device at 20 mA current has low correlation color temperature (CCT = 3608 K) and high color rendering index (Ra = 90.1), which can significantly improve the electroluminescence performance of cold WLED devices. These results indicate that the $K_3MoO_2F_5{\cdot}2H_2O{:}Mn^{4+}$ phosphor has potential application value in warm WLED excited by blue light chip.

Keywords

Mn^{4+}, Green Synthesis, Phosphor, WLED

1. Introduction

Compared with traditional incandescent lamp and fluorescent lamp, white light emitting diode (WLED) has the advantages of low heat, low power consumption, fast response, long life and so on [1] [2]. However, for the traditional WLED device with yellow $Y_3Al5O_{12}{:}Ce^{3+}$ (YAG: Ce) phosphor excited by blue InGaN chip, due to the lack of red light components, there are problems of high correlation color temperature(CCT, CCT > 4500 K) and low color rendering index (CRI, Ra < 80) [3]. Mn^{4+} activated phosphors have been reported for a variety of fluoride and oxide substrates [4] [5] [6] [7] [8]. However, Mn^{4+} doped oxide red phosphors usually require a high temperature solid phase method, which makes production expensive [9] [10]. Moreover, the strongest excitation peak of such phosphors is in the ultraviolet (UV) region rather than the blue region, resulting in a poor match with the blue LED chip. Compared with Mn^{4+} doped oxide phosphors, Mn^{4+} doped fluoride red phosphors can not only be synthesized under mild conditions, but also be effectively excited by blue LED chips. However, the synthesis of these phosphors requires highly toxic HF as a solvent, which will not only harm our bodies but also cause environmental pollution [11] [12]. Therefore, finding a green route is an important challenge in the synthesis of Mn^{4+} activated fluoride red phosphors. Wang *et al.* [13] synthesized $K_2XF_6:Mn^{4+}$ (X = Ti, Si, Ge) series samples by partially replacing HF with acetic acid. However, the use of acetic acid reduced the solubility of K_2XF_6, and $KMnO_4$ was prone to decomposition under heat, resulting in a low effective doping concentration of Mn^{4+} in the matrix and a decrease in luminescence intensity. Kumar *et al.* [14] proposed a new HF free and environmentally friendly closed solid phase method for the preparation of $K_2TiF_6:Mn^{4+}$ narrow band red luminescent material, which has higher color purity and lower color temperature, but its reaction conditions are harsh. In this work, $K_3MoO_2F_5 \cdot 2H_2O:Mn^{4+}$ phosphor was synthesized with low toxicity (NH_4HF_2 + HCl) instead of highly toxic HF. The crystal phase structure, morphology and element composition of the phosphor was discussed, and the spectral characteristics of the phosphor were analyzed in detail. Finally, the prepared $K_3MoO_2F_5 \cdot 2H_2O:Mn^{4+}$ red phosphors were assembled into WLEDs. The results show that $K_3MoO_2F_5 \cdot 2H_2O:Mn^{4+}$ phosphor prepared by green route is an ideal material for improving the performance of WLEDs.

2. Experimental

2.1. Chemical Regents

$KMnO_4$ (99.5%), KF (99%), HF (40 wt%), H_2O_2 (30%), MoO_3 (99.5%), KOH (85%), NH_4HF_2 and HCl. All reagents were purchased from the Shanghai Macklin Biochemical Co. Ltd. and were used directly without further purification. K_2MnF_6 was prepared as a manganese source by the strategy shown in **Figure 1** [15].

2.2. Maintaining Synthesis Process of $K_3MoO_2F_5 \cdot 2H_2O:Mn^{4+}$

The $K_3MoO_2F_5 \cdot 2H_2O:Mn^{4+}$ phosphor was prepared by a simple co-precipitation method with low toxicity (NH_4HF_2 + HCl) instead of highly toxic HF. Typically, the preparation details of $K_3MoO_2F_5 \cdot 2H_2O:Mn^{4+}$ phosphor are as follows (**Figure 2**). Firstly, 0.2822 g MoO_3 is completely dissolved in the 5 mL prepared KOH

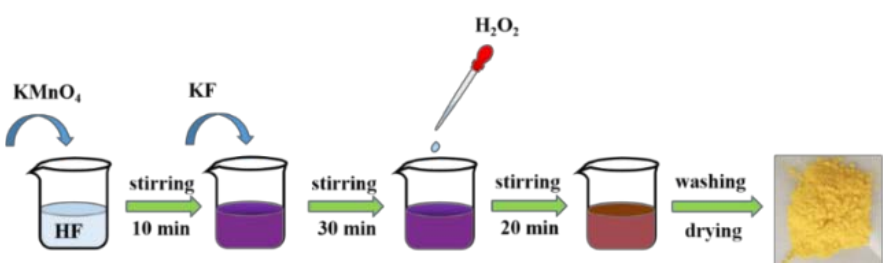

Figure 1. Diagram of the preparation process of K_2MnF_6.

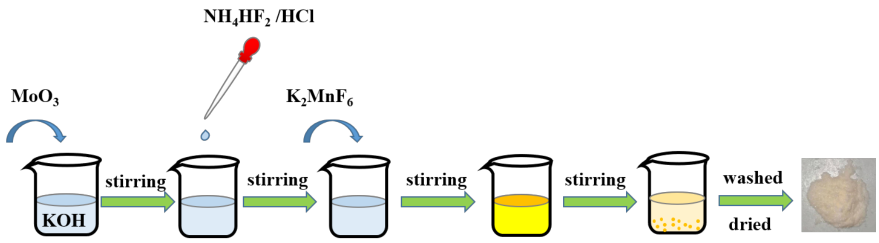

Figure 2. Diagram of the preparation process of $K_3MoO_2F_5{\cdot}2H_2O{:}Mn^{4+}$.

(1.6 mol·L^{-1}) solution. Subsequently, 0.4563 g NH_4HF_2 was added into 10 mL HCl solution (4 mol·L^{-1}), and this solution was added dropwise to the above solution. After 30 min of magnetic stirring, 0.0099 g K_2MnF_6 was added to the reacted solution and continued magnetic stirring for 30 min, a yellow precipitate was formed. Finally, the target product was obtained by centrifugation, washing with ethanol three times and drying at 60˚C for 6 h.

2.3. Fabrication of LED Devices

The warm white LED device was fabricated by mixing the as-synthesized red phosphor, yellow (YAG:Ce^{3+}) emitting commercial phosphor and organic silica gel A and B (a mass ratio of 1:4) with a blue LED chip (0.4 W, 460 nm), the mass ratio of yellow phosphor to red phosphor is 1:8. The integrating sphere LED photoelectric parameter comprehensive test system (SSP6612) was used to measure the photoelectric performances including the color rendering index, correlation color temperature electroluminescence (EL) spectra and CIE color coordinates of the fabricated LED devices.

2.4. Materials Characterization

The crystal structure of the phosphor was characterized via RigakuD/max - RA X-ray diffraction (XRD) with Cu Kα radiation (λ = 0.15406 nm) in the scanning range from 10˚ to 90˚ and the scanning speed was 6˚ min^{-1}. The morphology and composition of the sample was identified via JEOL JSM-7610F field emission scanning electron microscope (FE-SEM) and OXFORD ISIS-300 energy dispersive spectrometer (EDS). Using barium sulfate as the substrate, the UV-visible diffuse reflectance spectrum (DRS) of the phosphor was measured by Shimadzu UV-2550 spectrophotometer, in which the mode of the integrating sphere was set to external. Using the light source of 150 W xenon lamp as excitation source, the photoluminescence excitation (PLE) spectra, photoluminescence (PL) spectra of the sample was collected by HITACHI F-7000 fluorescence spectrophotometer in natural environment.

3. Results and Discussion

3.1. Structure, Morphology and Composition

The crystal phase structure and purity of the sample can be examined by XRD. **Figure 3** shows the XRD pattern of the as-prepared $K_3MoO_2F_5{\cdot}2H_2O{:}Mn^{4+}$ red

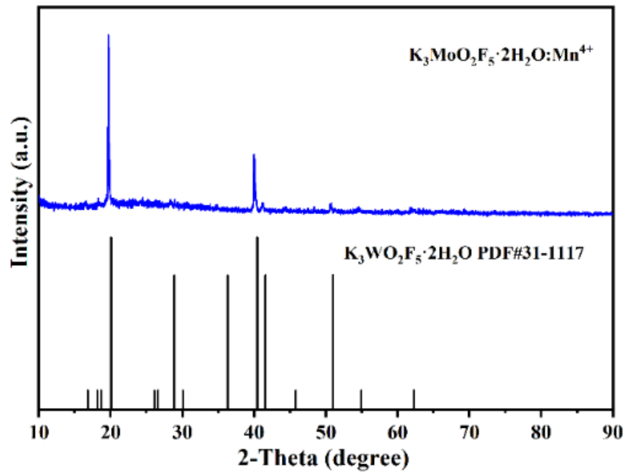

Figure 3. XRD pattern of $K_3MoO_2F_5·2H_2O:Mn^{4+}$.

phosphor by the co-precipitation method. It can be seen that the as-obtained diffraction peaks can be better corresponded with the standard card (PDF# 31-1117). The Mo^{6+} ion and Mn^{4+} ion have similar ionic radius and the same coordination number (($R_{Mo}{}^{6+}$ = 0.59 Å, $R_{Mn}{}^{4+}$ = 0.53 Å and CN = 6), thus rendering it possible the doping of Mn^{4+} does not influence significantly on the crystal structure of $K_3MoO_2F_5·2H_2O$. SEM image (a) and EDS spectrum (b) of $K_3MoO_2F_5·2H_2O:Mn^{4+}$ can be seen from **Figure 4**. The image shows that the phosphor is irregular lump with an average particle size of 70 - 100 μm and has a rough surface. As show in **Figure 4(b)**, the presence of K, Mo, O, F, Mn elements can be clearly observed. The above results show that the $K_3MoO_2F_5·2H_2O:Mn^{4+}$ phosphor was successfully synthesized by the co-precipitation method.

3.2. Photoluminescence Property

Figure 5(a) shows the excitation and emission spectra of phosphor respectively. When 632 nm was used as the monitoring wavelength, there were two obvious wide absorption bands in the wavelength range of 300 - 550 nm, and the centers of the absorption bands were located at 374 nm (UV region) and 470 nm (blue region), respectively. These two absorption bands are derived from the spin-allowing $^4A_{2g} \rightarrow {}^4T_{1g}$ and $^4A_{2g} \rightarrow {}^4T_{2g}$ energy level transitions of Mn^{4+}, respectively. The DRS of $K_3MoO_2F_5·2H_2O:Mn^{4+}$ (**Figure 5(b)**) shows that the phosphor has strong absorption in the blue region. In addition, the absorption peak also appears in the ultraviolet region at 270 nm, which can be attributed to the O/F → Mo charge transfer band in the matrix. At 470 nm excitation, the emission spectrum of $K_3MoO_2F_5·2H_2O:Mn^{4+}$ phosphor consists of seven typical emission peaks of Mn^{4+}, 600 nm, 611 nm and 615 nm correspond to anti-Stokes ν_3 (t_{1u}), ν_4 (t_{1u}) and ν_6 (t_{2u}) vibration models of Mn^{4+}, respectively. Stokes vibration model ν_6 (t_{2u}), ν_4 (t_{1u}) and ν_3 (t_{1u}) of Mn^{4+} correspond to emission peaks at 632 nm, 636 nm and 649 nm in the spectrum, among which 632 nm is the strongest emission peak. The characteristic emission peak at 624 nm is strong zero phonon line (ZPL) emission. This is due to the octahedral distortion caused by the nonequivalent substitution and the low symmetry of the crystal structure, so the strength of the ZPL is strong. **Figure 5(c)** is the CIE coordinate diagram of $K_3MoO_2F_5{\cdot}2H_2O{:}Mn^{4+}$ phosphor excited by 470 nm blue light. It can be seen that its coordinate is located at (0.6808, 0.3190), close to the NTSC ideal red coordinate point (0.67, 0.33). The illustration shows the phosphor under sunlight and UV-light irradiation respectively. It can be seen from the figure that the phosphor emits bright red light under UV-light irradiation. The color purity of phosphor is an important parameter to evaluate its color characteristics. The color purity of $K_3MoO_2F_5{\cdot}2H_2O{:}Mn^{4+}$ red phosphor is calculated as 98% by Equation (1) [16].

$$\text{Color purity} = \frac{\sqrt{(x-x_i)^2+(y-y_i)^2}}{\sqrt{(x_d-x_i)^2+(y_d-y_i)^2}} \tag{1}$$

where, (x_i, y_i) is the color coordinate of equal energy white light (0.33, 0.33), and (x_d, y_d) is the color coordinate of the strongest emission wavelength of the light source (0.6851, 0.3148). (x, y) represents the color coordinate of $K_3MoO_2F_5{\cdot}2H_2O{:}Mn^{4+}$ sample (0.6808, 0.3190). Obviously, all the emission peaks of oxyfluorides are located in sensitive areas that can be observed by the human eye. The excellent

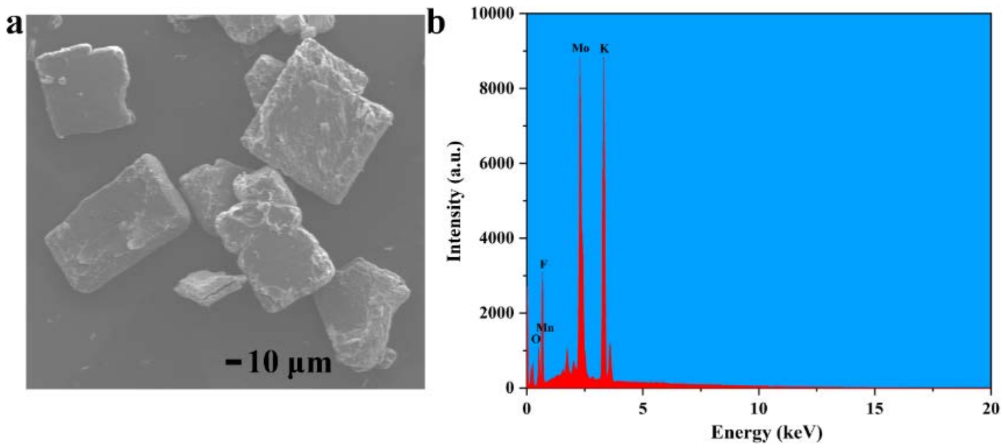

Figure 4. SEM image (a) and EDS spectrum (b) of $K_3MoO_2F_5{\cdot}2H_2O{:}Mn^{4+}$.

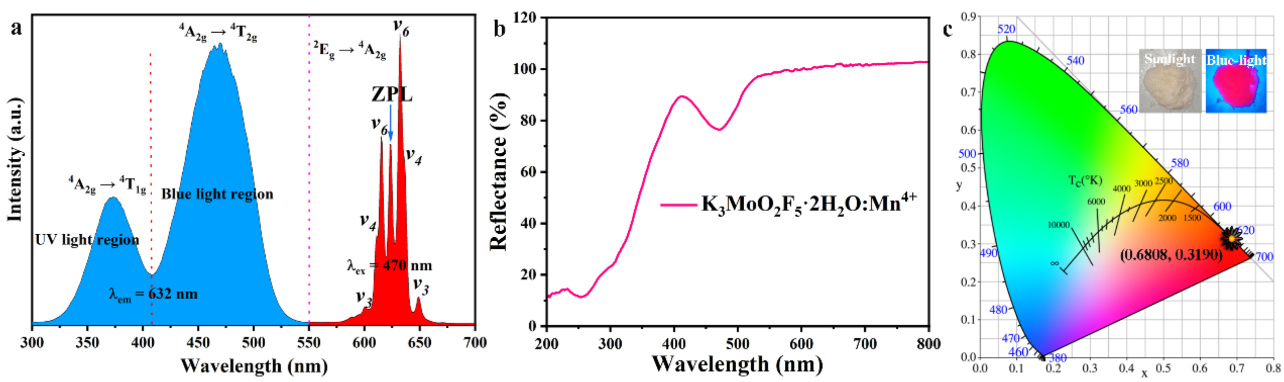

Figure 5. PLE and PL spectra (a), DRS (b) and CIE color coordinate and digital photos under natural light and ultraviolet light irradiation (c) of $K_3MoO_2F_5{\cdot}2H_2O{:}Mn^{4+}$.

optical properties of phosphor indicate that $K_3MoO_2F_5·2H_2O:Mn^{4+}$ red phosphor has potential application value in warm white LED.

3.3. Application of $K_3MoO_2F_5·2H_2O:Mn^{4+}$ Phosphor in Warm WLED

In order to explore the value of $K_3MoO_2F_5·2H_2O:Mn^{4+}$ red phosphor in practical applications, a series of WLED devices were packaged by combining blue chip (a) with yellow YAG:Ce^{3+} phosphor (b), red $K_3MoO_2F_5·2H_2O:Mn^{4+}$ phosphor (c) yellow YAG:Ce^{3+} phosphor + red $K_3MoO_2F_5·2H_2O:Mn^{4+}$ phosphor (d) mixed phosphor. **Figures 6(a)-(d)** show the electroluminescence spectra of the corresponding LED devices at 20 mA driving current. The characteristic emission at 430 - 470 nm is that of blue chip. The 470 - 590 nm range belongs to the emission peak of YAG:Ce^{3+} yellow phosphor. In the range of 590 - 660 nm, there is obvious red emission, indicating that the $K_3MoO_2F_5·2H_2O:Mn^{4+}$ phosphor can be well excited by blue chip and emit strong red light. Due to the lack of red light component, the cold WLED device has a higher relative color temperature (CCT = 5190 K) and a lower color rendering index (Ra = 70.4), and its LE is 120.07 $lm·W^{-1}$. In order to improve this problem, the red light component was introduced into the WLED device, and the CCT of the device was reduced to 3608 K, the CRI was increased to 90.1, and the LE was 50.17 $lm·W^{-1}$. At the same time, CIE coordinate of the cold WLED was transferred from (0.3536, 0.3960) to (0.4069, 0.3681) in the warm WLED region (**Figure 6(e)**). The above results show that the device obtained is more suitable for the application of warm WLED device in indoor lighting field. **Table 1** lists the photoelectric performance parameters of each device in detail.

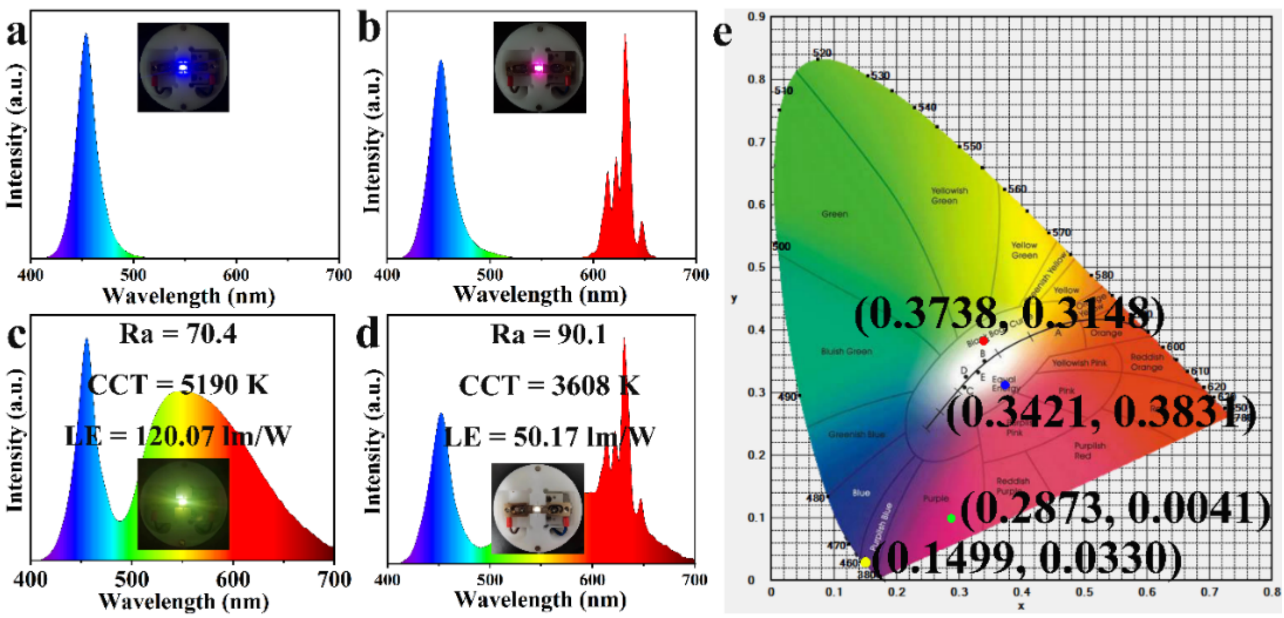

Figure 6. Electroluminescence (EL) spectra and digital photos and CIE color coordinates (e) excited by the current of 20 mA of GaN chip (a), GaN chip + red $K_3MoO_2F_5·2H_2O:Mn^{4+}$ phosphor (b), GaN chip + yellow YAG:Ce^{3+} phosphor (c), GaN chip + yellow YAG:Ce^{3+} phosphor + red $K_3MoO_2F_5·2H_2O:Mn^{4+}$ phosphor (d).

Table 1. Important photoelectric parameters of the LED devices under 20 mA.

Device	Current (mA)	R_a	T_c (K)	CIE (x, y)	R_9	Luminous efficiency ($lm \cdot W^{-1}$)
GaN Chip	20	0	25000	(0.1499, 0.0330)	−207	20.88
GaN Chip + YAG:Ce^{3+}	20	70.4	5190	(0.3421, 0.3831)	−47	120.07
GaN Chip + $K_3MoO_2F_5 \cdot 2H_2O:Mn^{4+}$	20	0	25000	(0.2873, 0.0041)	−595	7.83
GaN Chip + YAG:Ce^{3+} + $K_3MoO_2F_5 \cdot 2H_2O:Mn^{4+}$	20	90.1	3608	(0.3738, 0.3148)	79	50.17

4. Conclusion

$K_3MoO_2F_5 \cdot 2H_2O:Mn^{4+}$ phosphor was prepared using (NH_4HF_2 + HCl) instead of highly toxic HF. Under 470 nm blue light excitation, $K_3MoO_2F_5 \cdot 2H_2O:Mn^{4+}$ phosphor shows narrow-band red emission. The emission peak ranges from 580 nm to 670 nm, which is attributed to the $^2E_g \rightarrow {}^4A_{2g}$ level transition prohibited by the spin of Mn^{4+}. Efficient warm WLED with low CCT (3608 K), high CRI (Ra = 90.1) and LE of 50.17 $lm \cdot W^{-1}$ were obtained using $K_3MoO_2F_5 \cdot 2H_2O:Mn^{4+}$ as red light component. These results indicate that phosphor $K_3MoO_2F_5 \cdot 2H_2O:Mn^{4+}$ has potential application value in warm WLED.

Acknowledgements

This work was financially supported by the National Natural Science Foundation of China (51802027).

Conflicts of Interest

The authors declare no conflicts of interest regarding the publication of this paper.

References

[1] Jiang, C.Y., Brik, M.G., Li, L.H., Li, L.Y., Peng, J., Wu, J.N., Molokeew, M.S., Wong, K.L. and Peng, M.Y. (2018) Electronic and Optical Properties of Narrow-Band-Emitting Red Nanophosphor K_2NaGaF_6: Mn^{4+} for Warm White Light-Emitting Diodes. *Journal of Materials Chemistry C*, **6**, 3016-3025. https://doi.org/10.1039/C7TC05098D

[2] Yu, Y., Wang, T.M., Deng, D.S., Zhong, X., Li, Y.L., Wang, L., Liao, S., Huang, Y.H. and Long, J.Q. (2022) Enhancement of the Luminescent Thermal Stability and Water Resistance of $K_2SiF_6:Mn^{4+}$, Na^+ by Double Coating of GQDs and K_2SiF_6. *Journal of Alloys and Compounds*, **898**, Article ID: 162819. https://doi.org/10.1016/j.jallcom.2021.162819

[3] Xie, Z.X., Tong, J.Z., Li, L., Hong, F., Chen, J.Y., Yang, J.Y. and Lin, H. (2023) Green Synthesis Strategy to Construct Strong Zero-Phonon Line Red Emission Phosphor $Na_2SiF_6:Mn^{4+}$: Photoluminescence Properties, Thermal Stability and Application in Warm White LEDs. *Journal of Luminescence*, **257**, Article ID: 119684.

https://doi.org/10.1016/j.jlumin.2023.119684

[4] Huang, L., Liu, Y., Yu, J.B., Zhu, Y.W., Pan, F.J., Xuan, T.T., Brik, M.G., Wang, C.X. and Wang, J. (2018) Highly Stable $K_2SiF_6:Mn^{4+}$ @K_2SiF_6 Composite Phosphor with Narrow Red Emission for White LEDs. *ACS Applied Materials & Interfaces*, **10**, 18082-18092. https://doi.org/10.1021/acsami.8b03893

[5] Lin, H., Hu, T., Huang, Q.M., Cheng, Y., Wang, B., Xu, J., Wang, J.M. and Wang, Y.S. (2017) Non-Rare-Earth $K_2XF_7:Mn^{4+}$ (X = Ta, Nb): A Highly-Efficient Narrow-Band Red Phosphor Enabling the Application in Wide-Color-Gamut LCD. *Laser & Photonics Reviews*, **11**, Article ID: 1700148. https://doi.org/10.1002/lpor.201700148

[6] Gao, J., Zhu, H.M., Li, R.F., Huang, D.C., Luo, B.L., You, W.W., Ke, J.X., Yi, X.D., Shang, X.Y., Xu, J., Deng, Z.H., Xu, L., Guo, W. and Chen, X.Y. (2019) Moisture-Resistant and Highly Efficient Narrow-Band Red-Emitting Fluoride Phosphor $K_2NaGaF_6:Mn^{4+}$ for Warm White LED Application. *Journal of Materials Chemistry C*, **7**, 7906-7914. https://doi.org/10.1039/C9TC02445J

[7] Zhu, Y., Zhao, S.N., Wang, J.L. and Zhang, N.M. (2023) Al^{3+} Ions Co-Doped $Ba_2YSbO_6:Mn^{4+}$ Phosphors with High Thermal Stability and Strong Far-Red Emission for Plant Growth LEDs. *Journal of Solid State Chemistry*, **320**, Article ID: 123854. https://doi.org/10.1016/j.jssc.2023.123854

[8] Wang, W.H., Li, Q.F., Chen, L.Y., Wang, Y.H., Zhong, Dong, H.W., Qiu, Y.J., Hu, Y.F. and Zhang, X.L. (2023) Red Emitting $Ba_2LaNbO_6:Mn^{4+}$ Phosphor for the Lifetime-Based Optical Thermometry. *Journal of Luminescence*, **257**, Article ID: 119683. https://doi.org/10.1016/j.jlumin.2023.119683

[9] Li, Z.Y., Zhang, X.H., Wu, J., Guo, R., Luo, L., Xiong, Y.H., Wang, L. and Chen, W. (2021) A Novel Inequivalent Double-site Substituted Red Phosphor $Li_4AlSbO_6:Mn^{4+}$ with High Color Purity: its Structure, Photoluminescence Properties, and Application in Warm White LEDs. *Journal of Materials Chemistry C*, **9**, 13236-13246. https://doi.org/10.1039/D1TC02541D

[10] Zhang, Y.L., Hu, S., Liu, Y.L., Wang, Z.J., Zhou, G.H. and Wang, S.W. (2018) Red-Emitting $Lu_3Al_5O_{12}$:Mn Transparent Ceramic Phosphors: Valence State Evolution Studies of Mn Ions. *Ceramics International*, **44**, 23259-23262. https://doi.org/10.1016/j.ceramint.2018.08.293

[11] Zhou, Y.Y., Song, E.H., Deng, T.T. and Zhang, Q.Y. (2018) Waterproof Narrow-Band Fluoride Red Phosphor $K_2TiF_6:Mn^{4+}$ via Facile Super-Hydrophobic Surface Modification. *ACS Applied Materials & Interfaces*, **10**, 880-889. https://doi.org/10.1021/acsami.7b15503

[12] Fang, Z.Y., Lai, X.H., Zhang, J. and Zhang, R. (2021) Surface Modification of $K_2TiF_6:Mn^{4+}$ Phosphor with SrF_2 Coating to Enhance Water Resistance. *International Journal of Applied Ceramic Technology*, **18**, 1106-1113. https://doi.org/10.1111/ijac.13751

[13] Wang, Z.L., Zhou, Y.Y., Yang, Z.Y., Liu, Y., Yang, H., Tan, H.Y., Zhang, Q.H. and Zhou, Q. (2015) Synthesis of $K_2XF_6:Mn^{4+}$ (X=Ti, Si and Ge) Red Phosphors for White LED Applications with Low-Concentration of HF. *Optical Materials*, **49**, 235-240. https://doi.org/10.1016/j.optmat.2015.09.023

[14] Kumar, V., Potdevin, A., Boutinaud, P. and Boyer, D. (2019) HF-Free Synthesis of K_2SiF_6 and $BaSiF_6$ Nanoparticles by Thermal Decomposition. *Materials Letters*, **261**, Article ID: 127123. https://doi.org/10.1016/j.matlet.2019.127123

[15] Liu, X.Y., Hong, F., Pang, G., Cheng, H.M., Yu, X.S., Wang, H., Liu, G.X., Li, D., Dong, X.T., Wang, J.X. and Yu, W.S. (2022) A Novel $K_3WO_2F_5\cdot 2H_2O:Mn^{4+}$ Phosphor with Excellent Hydrophobic Stability by Coating Paraffin Wax for the Appli-

cation of WLEDs. *Journal of Alloys and Compounds*, **918**, Article ID: 165522. https://doi.org/10.1016/j.jallcom.2022.165522

[16] Hong, F., Yang, L., Xu, H.P., Chen, Z.Y., Liu, Q.X., Liu, G.X., Dong, X.T. and Yu, W.S. (2019) A Red-Emitting Mn^{4+} Activated Phosphor with Controlled Morphology and Two-Dimensional Luminescence Nanofiber Film: Synthesis and Application for High-Performance Warm White Light-Emitting Diodes (WLEDs). *Journal of Alloys and Compounds*, **808**, Article ID: 151551. https://doi.org/10.1016/j.jallcom.2019.07.263